Surveys in Geophysics (2021) 42:727–755
https://doi.org/10.1007/s10712-021-09637-5

Using Satellite Data for CBRN (Chemical, Biological, Radiological, and Nuclear) Threat Detection, Monitoring, and Modelling

Gary Sutlieff[1] · Lucy Berthoud[2] · Mark Stinchcombe[2]

Received: 19 November 2020 / Accepted: 23 February 2021 / Published online: 17 April 2021

Abstract
CBRN (Chemical, Biological, Radiological, and Nuclear) threats are becoming more prevalent, as more entities gain access to modern weapons and industrial technologies and chemicals. This has produced a need for improvements to modelling, detection, and monitoring of these events. While there are currently no dedicated satellites for CBRN purposes, there are a wide range of possibilities for satellite data to contribute to this field, from atmospheric composition and chemical detection to cloud cover, land mapping, and surface property measurements. This study looks at currently available satellite data, including meteorological data such as wind and cloud profiles, surface properties like temperature and humidity, chemical detection, and sounding. Results of this survey revealed several gaps in the available data, particularly concerning biological and radiological detection. The results also suggest that publicly available satellite data largely does not meet the requirements of spatial resolution, coverage, and latency that CBRN detection requires, outside of providing terrain use and building height data for constructing models. Lastly, the study evaluates upcoming instruments, platforms, and satellite technologies to gauge the impact these developments will have in the near future. Improvements in spatial and temporal resolution as well as latency are already becoming possible, and new instruments will fill in the gaps in detection by imaging a wider range of chemicals and other agents and by collecting new data types. This study shows that with developments coming within the next decade, satellites should begin to provide valuable augmentations to CBRN event detection and monitoring.

Article Highlights
- There lite data in fields that are of interest to CBRN detection and monitoring.
- The data is mostly of insufficient quality (resolution or latency) for the demanding requirements of CBRN modelling for incident control.
- Future technologies and platforms will improve resolution and latency, making satellite data more viable in the CBRN management field

✉ Gary Sutlieff
gary.sutlieff@bristol.ac.uk

[1] Department of Aerospace Engineering, University of Bristol, Bristol BS8 1TR, UK

[2] Thales Alenia Space UK, Building 660, Business Park, Coldharbour Ln, Stoke Gifford, Bristol BS16 1EJ, UK

Keywords CBRN · Satellite · Earth observation · Monitoring · Detection

1 Introduction

CBRN, or chemical, biological, radiological, and nuclear, is a label applied to hazardous events of a chemical, biological, radiological, or nuclear nature, in which an agent such as a chemical or a virus, or simply radiation, is dispersed into an area and poses a risk to individuals lives or health.

The threat of CBRN events is an ever growing one in the modern world, brought to light by recent high-profile incidents such as the leaks from the Fukushima Daiichi Nuclear Plant following the earthquake which spread irradiated seawater into the pacific (World Nuclear Association 2020), and the release of the Novichok nerve agent in Salisbury (Carlsen 2018). Chemical weapons are confirmed to have been used in Syria (Wojtas and European Commission DG Home Affairs 2018), and intelligence indicates that organisations such as Daesh/ISIS have the capability to produce and use such weapons (Houses of Parliament 2019). CBRN incidents are difficult to manage or contain safely, since the agents involved are often invisible to the eye, lethal or otherwise highly hazardous, and can disperse over wide areas within short amounts of time (Houses of Parliament 2019).

CBRN events have the potential for high casualty numbers and therefore require rapid responses from multi-agency teams featuring specialised personnel and equipment. Coordination is needed to minimise casualties among civilians and the response team (Joint Emergency Services Interoperability Programme (JESIP) 2016). Responders therefore need effective situational awareness and hazard prediction. Any tools that can provide these will be of great value, and data from satellites can be useful in producing more accurate models and simulations to match the critical nature of these threats. Current models do not heavily rely or draw on satellite data, except for weather information and some land use maps and building height data. A 2011 CBRN case study from the Centre for Strategy and Evaluation Services indicated that the integration of satellite surveillance data was an area for further research (Centre for Strategy and Evaluation Services 2011).

New sensors and instrumentation are becoming available, and new platforms and missions to support these instruments are becoming possible. Additionally, the capabilities for high-resolution observations have improved over the past few years, allowing for improvements on existing model fidelity and utility. Using this information to improve inputs to CBRN modelling tools will produce valuable training and incident management capabilities to help combat CBRN events as they occur (Selva and Krejci 2012).

Section 2 of this review details currently available satellite data that is of relevance to the CBRN field, providing examples of the spatial resolutions and latencies that can be expected for different instruments, satellites, and data types. Section 3 highlights the gaps in the data presented in Sect. 2, and the areas in which satellites and satellite data can be improved for CBRN purposes. Section 4 describes several emergent technologies in development or implementation that will fill in some of the gaps presented in Sect. 3, and Sect. 5 lists examples of upcoming missions and instruments that will provide new data to consider for CBRN applications. Section 6 provides the conclusions of the paper.

2 Currently Available Satellite Data

2.1 Chemical Detection and Sounding

2.1.1 Chemical Detection

Where CBRN event detection is concerned, having the capability to detect Chemical Warfare Agents (CWAs) or Toxic Industrial Chemicals (TICs) using satellites would naturally be valuable, potentially allowing for rapid detection of an incident and identification of the chemicals involved, provided sufficient satellite coverage. However, the range of chemicals that can be detected and monitored from space is mainly focused on gases with noticeable effects on overall climate, such as ozone and various greenhouse gases including the carbon, sulphur and nitrogen oxides (Gonzalez Abad et al. 2019). Some commonly monitored gases may be relevant to CBRN purposes, such as the sulphur and nitrogen oxides, formaldehyde, and hydrogen cyanide (Gonzalez Abad et al. 2019; Pumphrey et al. 2018).

Methane is another chemical that is a focus of monitoring efforts. Historical satellites and instruments such as EO-1′s Hyperion have imaged methane emissions from space, as shown in Fig. 1 (NASA 2016).

While EO-1 is no longer active, other instruments such as TROPOMI on Sentinel-5P can detect methane leaks, and in the future start-ups such as Bluefield have imaged Methane with microsatellites (Bluefield 2020b). Figure 2 is a sample of what such imaging could look like (Bluefield 2020a).

Many different chemicals are observed from space beyond these examples, and since chemical detection from space typically involves the use of laser reflectance spectroscopy

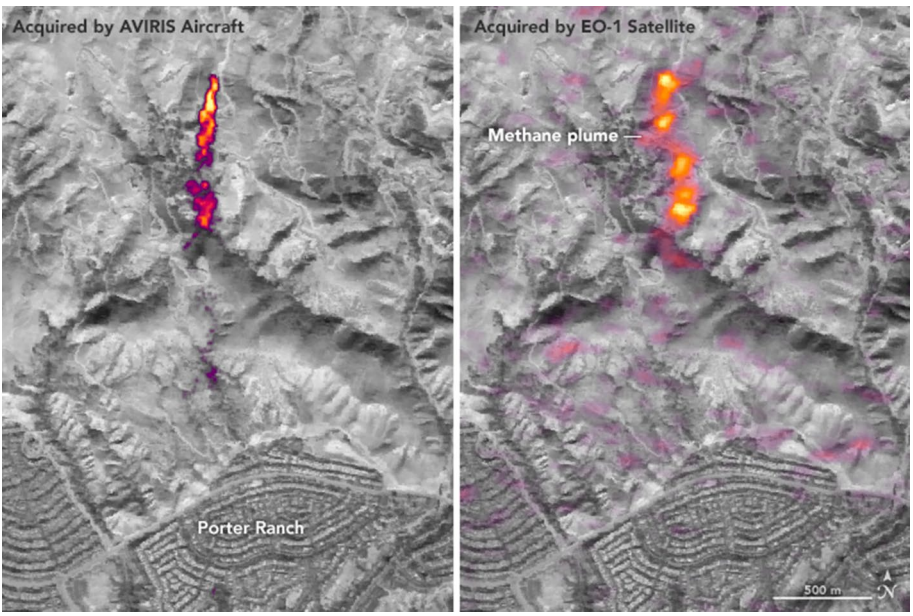

Fig. 1 Methane plumes from a large underground natural gas storage facility near Porter Ranch, California, detected by EO-1′s Hyperion instrument in 2016

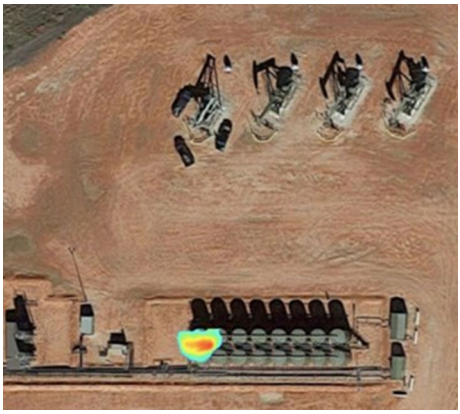

Fig. 2 Sample methane image from Bluefield, a start-up focused entirely on satellite methane monitoring

at a wavelength that matches the target chemical's absorption bands (Gonzalez Abad et al. 2019), which is a kind of sounding as described in Sect. 2.1.2, it is possible to image any chemical with use of the appropriate wavelength, if said wavelength is not absorbed by the atmosphere such as gamma wavelengths. However, this would require either specific instruments operating at these wavelengths or a new instrument that varies its imaging wavelength to observe a wider range of chemicals, as well as the capability to distinguish the target chemical from others that interfere with the observations.

Chemical detection from satellites is also focused on the stratosphere and upper troposphere, though lower altitude detections are possible, with some relevant cases to CBRN purposes such as separating aerosol smoke from clouds (Gupta and Follette-Cook 2017). In general, chemical detection from space presents an area for improvement, as discussed in Sect. 3.6.

2.1.2 Sounding

Sounding, or atmospheric column measurement, is a method in which vertical profiles of either temperature or moisture are retrieved from radiance measurements (NOAA OSPO 2014). The Metop Satellites and several of the NOAA satellites are equipped with the MHS, or Microwave Humidity Sounder, and the Advanced Microwave Sounding Units (AMSUs) on older satellites, which measure the radiance in the microwave spectrum to produce vertical measurements of humidity and water content with the exception of small ice particles which are transparent to microwave frequencies (EUMETSAT 2020a).

These satellites also have the High-resolution Infra-Red Sounder, or HIRS, which measures scene radiance to calculate a vertical temperature profile for the earth down to 45 km in height, when combined with readings from AMSU-A, which is also on those satellites (Emery and Camps 2017). Readings of the atmospheric temperature at different heights can also be derived from these measurements, and maps can be produced of temperature at a given pressure, which corresponds to a particular height, with a 40 km horizontal resolution (NOAA Office of Satellite and Product Operations 2017). Vertical sounding profiles for temperature and moisture can act as inputs for long-term monitoring or modelling of an incident that propagates over large distances in the atmosphere, though the limits in both resolution and the depth into the atmosphere of the measurements mean that technological

improvements will be needed before this data is useful for monitoring the majority of incidents.

2.2 Meteorological

A wide range of meteorological data is retrieved by satellites, including wind velocity vectors and cloud properties such as optical depth, as well as weather data such as precipitation (ESA EO Directory 2020). These observations are largely focused on the atmosphere at cloud height or above, though this data could still hold much relevance to CBRN applications as inputs towards modelling how various environmental factors such as wind or precipitation could affect the spread of an agent.

2.2.1 Wind Velocity

Atmospheric Motion Vectors can be derived from satellite radiometry data by tracking clouds and other water vapour features. These describe the direction and velocity of wind. In Europe, data on these vectors is collected from four existing instruments: SEVERI, AVHRR, ASCAT and ALADIN.

The first instrument is the Spinning Enhanced Visible and InfraRed Imager, or SEVIRI, which is mounted on the MeteoSat Second Generation, or MSG, Satellites from MeteoSat 8 onwards. SEVIRI has a 50 cm aperture and 12 channels, 4 in visible and very near infrared, and 8 in infrared. One VNIR channel has a 1 km sampling distance, and all the others have a 3 km sampling distance, and the instrument images the full MSG disc in 1250 line scans from north to south, each line step being 9 kms wide (Schmid 2000). The resolution of the imager is 3 km at the sub-satellite point, or 1 km in the high-resolution visible channel (Schmid 2000). The latency of receiving the data is between 3 and 6 h (JPL 2020) (EUMETSAT 2020b).

The second instrument is the Advanced Very-High-Resolution Radiometer, AVHRR**,** on the Metop satellites. AVHRR has two channels in red visible light and near-infrared, and two more in the thermal infrared. AVHRR has a ground sampling distance between 1 and 4 km. The data is also averaged over 150 km resolution pixels for global mapping purposes (Borde, Hautecoeur and Carranza 2016). SEVIRI and AVHRR monitor wind vectors in the upper troposphere and sometimes the lower stratosphere.

Metop satellites also carry the ASCAT instrument, or Advanced Wind Scatterometer, which determines wind vector fields at the surfaces of the oceans by measuring the backscattering coefficient, or normalised radar cross section with a swath width of 500 km and a spatial resolution between 12.5 and 50 km (World Meteorological Organisation 2020).

More recently in 2018, the satellite ADM-Aeolus launched with the Atmospheric Laser Doppler Instrument, or ALADIN, which is a Doppler wind LiDAR. These work by emitting a laser beam that is reflected and backscattered by atmospheric aerosols that are carried along by the wind. Measurements of the Doppler shift on the backscattered beam can be used to determine the speed of these aerosol particles and therefore the wind carrying them (Stoffelen et al. 2005). ALADIN surveys the Earth in horizontal strips 87 km wide with a 3 km subsampling size (Straume et al. 2017), and a vertical resolution between 250 m and 2 km (Reitebuch 2008), and ALADIN also measures the wind velocity to within 2 ms^{-1} with a latency on obtaining the data of 3 h (Straume et al. 2017) (Reitebuch 2008). Figure 3 shows the first sample of Aeolus data to be released publicly by the European Space Agency (ESA 2018).

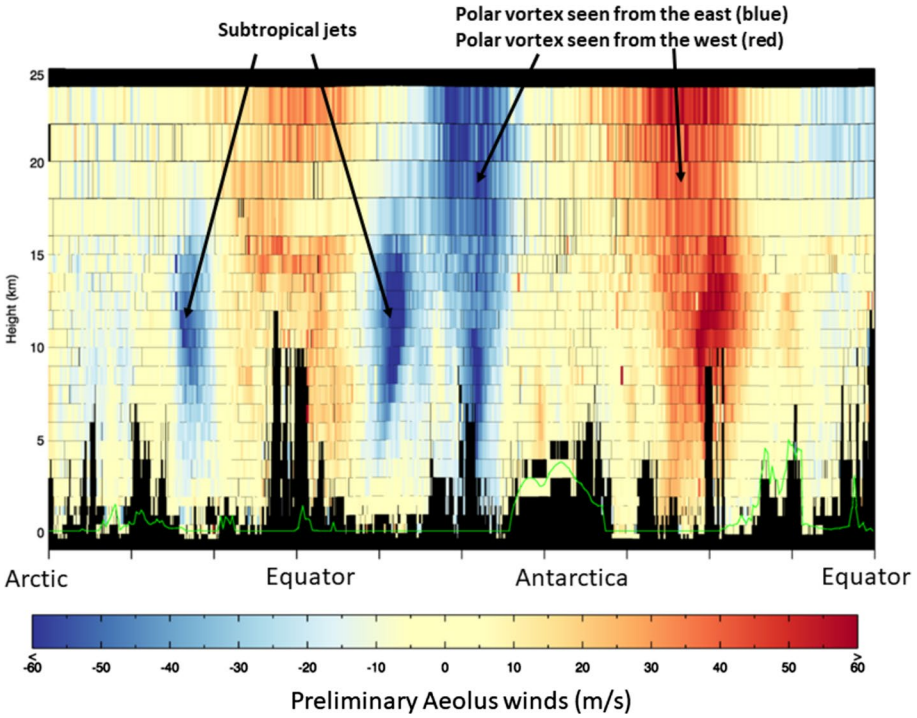

Fig. 3 First sample of Aeolus wind velocity data. Note the annotations pointing out polar vortices in the data, and the fact that the black areas show that the data collection is limited below around 2 km

This data may be difficult to interpret, but wind pattern features are discernible once it is clear what to look for. Access to the Aeolus data service publicly opened in Spring 2020.

Much of the wind velocity data is unfortunately of too coarse a resolution for reliable application to CBRN modelling, in which it would of course be used to model the wind-driven propagation of an agent. In addition, the data is only for higher altitudes, above where incidents will most likely take place. Aeolus partially solves the former of these problems, particularly in the vertical regime, but is still affected by the latter, as evidenced by Fig. 1. As such, most models utilise wind data from other sources that track closer to the ground (Global Wind Atlas 2020).

2.2.2 Cloud Properties

The European Organisation for the Exploitation of Meteorological Satellites, or EUMETSAT, collates data from several satellites through its Climate Monitoring Satellite Applications Facility, or CM SAF, producing maps detailing the cloud coverage as well as several cloud properties, including optical depth, phase, water path, and the cloud top pressures, temperatures, and heights (EUMETSAT CM SAF 2020). The CMSAF baseline imaging area is focused on Europe, covering latitudes between 30 and 80 degrees North, and longitudes between 60 degrees west and 60 degrees east. The pixel size is 15 by 15 kms, and images are available each day dating back to the 1 November 2004 (EUMETSAT CM SAF 2020).

Recently, information and data on cloud top height, temperature, and pressure have been updated to include data from the SEVIRI instrument on MeteoSat Second Generation, or MSG. These images cover a wider disc which features Europe, Africa and the Atlantic, and they have a spatial resolution of 0.05 degrees, which is equal to about 5.5 km. These images are also available daily as far back as the 1 November 2018 (EUMETSAT CM SAF 2020).

Unfortunately, the spatial resolution of these data products is insufficient to match the requirements of CBRN models, being on the scale of kilometres or even poorer. Furthermore, properties at cloud height may only be relevant to CBRN incidents in a limited sense, being at a significantly higher altitude than would be typical for a CBRN incident.

2.2.3 Precipitation

EUMETSAT also has a Satellite Applications Facility on Support to Operational Hydrology and Water Management, or H-SAF, which provides collated satellite data on precipitation levels (EUMETSAT H-SAF 2020). These images come in five types from different instruments, among which is SEVIRI (EUMETSAT H-SAF 2020). The data products cover the H-SAF area, which stretches between 25 and 75 degrees North, and 25 degrees West to 45 degrees East (EUMETSAT H-SAF 2020).

Three of these five data products map precipitation rate in millimetres per hour (EUMETSAT H-SAF 2020). One uses radiometers on the sun-synchronous DMSP, or Defense Meteorological Satellite Programme satellites, measuring in 1400 km swaths at 30 km spatial resolution (EUMETSAT H-SAF 2020). Up to six passes occur every day, and data can be obtained within 150 min of the observations (EUMETSAT H-SAF 2020). Another uses the Microwave Humidity Sounder, MHS, on the Metop and NOAA, or National Oceanic and Atmospheric Administration, satellites to measure in strips of 2250 km swaths at a resolution of 16 km. The data is available within 30 min of the observations (EUMETSAT H-SAF 2020).

The third uses images from Geostationary Infrared imaging satellites, specifically the SEVIRI instruments on the MSG satellites, to generate the precipitation maps, which are then calibrated using the data from the microwave imagers to produce higher resolution images (EUMETSAT H-SAF 2020). These cover the H-SAF disc extended to cover more of Africa and the southern Atlantic, between 60 degrees South and 67.5 degrees North, and 80 degrees West to 80 degrees East. The images are produced every 15 min at a resolution between 3 and 8 km over Europe. The images are also available within 5 min of the end of the real-time data acquisition (EUMETSAT H-SAF 2020). The fourth maps accumulated precipitation in 6-h intervals over the same area and to the same resolution, with images available in 3-h intervals, 15 min after production (EUMETSAT H-SAF 2020). Finally, the fifth image type is produced by the calibration method and maps the convective precipitation cells (EUMETSAT H-SAF 2020).

Precipitation data is useful for CBRN incident modelling and monitoring since weather conditions such as precipitation would likely affect the propagation of certain agents. However, much like other meteorological data presented in this section, the spatial resolution on a scale of km is too imprecise for the requirements of CBRN models.

2.3 Surface Properties

2.3.1 Humidity

The EUMETSAT Satellite Applications Facility for Land Surface Analysis, or LSA SAF, distributes data on several surface properties, among which is humidity (EUMETSAT LSA SAF 2020; Trigo et al. 2011).

The SEVIRI instrument on Meteosat can measure evapotranspiration rate, the rate at which water is transferred from the surface to the atmosphere by evaporation from the surfaces and transpiration from plants in millimetres per hour. The data product covers the region from 80 degrees West to East and North to South, or the full Meteosat Second Generation, or MSG, disc (EUMETSAT 2020b). Images are produced daily with a 30-min latency on data acquisition (EUMETSAT 2020b), and the ground spatial resolution is 3 km (Schmid 2000).

Additionally, the NOAA GOES or Geostationary Operational Environment Satellites measure provides radiance data that can be used to calculate relative humidity using various algorithms combining the data with results from the Terra satellites Moderate Resolution Imaging Spectrometer instrument, MODIS. These each provide a resolution between 1 and 5 km, averaging at around 4 km (Ramírez- Beltrán et al. 2019).

While CBRN modelling could make use of humidity in determining the propagation of an agent, the resolution of the data provided from these satellites is too coarse for CBRN applications.

2.3.2 Albedo

The LSA SAF also uses data from SEVIRI to provide maps of surface albedo across the MSG full disc at 3 km ground spatial resolution (EUMETSAT LSA SAF 2020) (EUMETSAT LSA SAF 2020). Data products are available either in a daily format or every ten days. The satellite applications facility also uses data from the Metop satellites AVHRR instrument to produce ten-daily time-composite images of surface albedo in a 1 km grid centred at 0 degrees North, 0 degrees West (EUMETSAT LSA SAF 2020).

Information from the MODIS instrument on NASA's Terra and Aqua satellites also provides data products of albedo measurements across the globe with spatial resolution between 500 m and 5.6 km, with most products of 1 km resolution. These products are integrated every 16 days using data from both satellites (University of Hamburg 2019).

While 1 km spatial resolution is closer to meeting modelling requirements than the resolution of other surface property data products, this is still insufficient. Furthermore, the slow product integration times of 10–16 days means that this data is not suitable for modelling during an incident response, only for simulations performed ahead of time. Additionally, surface optical properties such as albedo and emissivity can be necessary in radiometry or sounding-based chemical detection, since these techniques depend on a return signal reflected from the Earth.

2.3.3 Temperature

Surface temperature maps are available from LSA SAF using the same data sources as the albedo maps (EUMETSAT LSA SAF 2020). SEVIRI data in the thermal infrared is

used to produce retrievals of land surface temperature from the differential absorption. The resultant maps are of 3 km spatial resolution, as with all SEVIRI ground measurements, and cover the full MSG disc (EUMETSAT LSA SAF 2020; Freitas et al. 2010; Trigo et al. 2008; Göttsche et al. 2016). The measurements are accurate to within less than 2 degrees Celsius, and retrievals can in theory be made every 15 min, for 96 images every day, though due to cloud cover it is often fewer than this (EUMETSAT LSA SAF 2020). Furthermore, on a ten-daily basis, these images are synthesised into another data product of derived land surface temperature (EUMETSAT LSA SAF 2020).

Just as with Albedo, the AVHRR instrument also provides retrievals of land surface temperature, with global coverage and a resolution of 1 km. Images from AVHRR data are produced every half-day, so there are retrievals for both day- and night-time (EUMETSAT LSA SAF 2020).

Surface temperature is a useful property in calculating the state and propagation of an agent after its initial spread, but in this case the spatial and temporal resolutions are both insufficient to match the requirements of incident modelling and the more urgent need for data during a response.

2.4 Data Survey: Spatial Resolution Against Revisit Time

This section looks at spatial resolution and revisit time for past, current, and future predicted satellite data for various different instrument types, including Visible/Infrared imagers, Lidars, Hyperspectral imagers and Synthetic Aperture Radars. Figures 4, 5, 6 and 7 show data for Visible/Infrared, Lidar, Hyperspectral and SAR imagers, respectively. Please note that any data points marked with a hash are for upcoming instruments, any marked with an asterisk are historical instruments, and that the size of the data point bubble represents the mass of the spacecraft.

These figures demonstrate that satellites have widely varying resolutions and revisit times, but that SAR and visible imaging tends to provide the best resolutions. Revisit times are less consistent, though generally future systems such as Capella aim to have

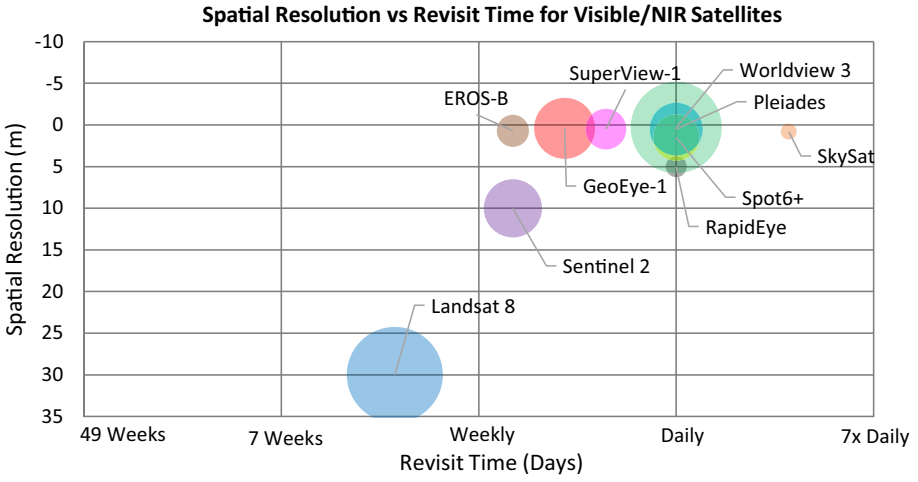

Fig. 4 A graph showing spatial resolution against revisit time for visible and near-infrared imaging satellites. Several of the imagers have spatial resolutions of one metre

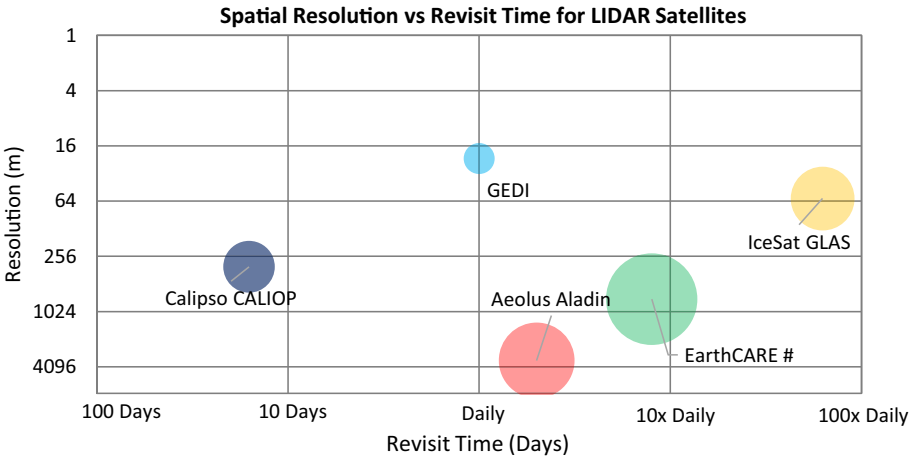

Fig. 5 Spatial resolution against revisit time for various LiDAR instruments. Note that EarthCARE is due to launch in 2022

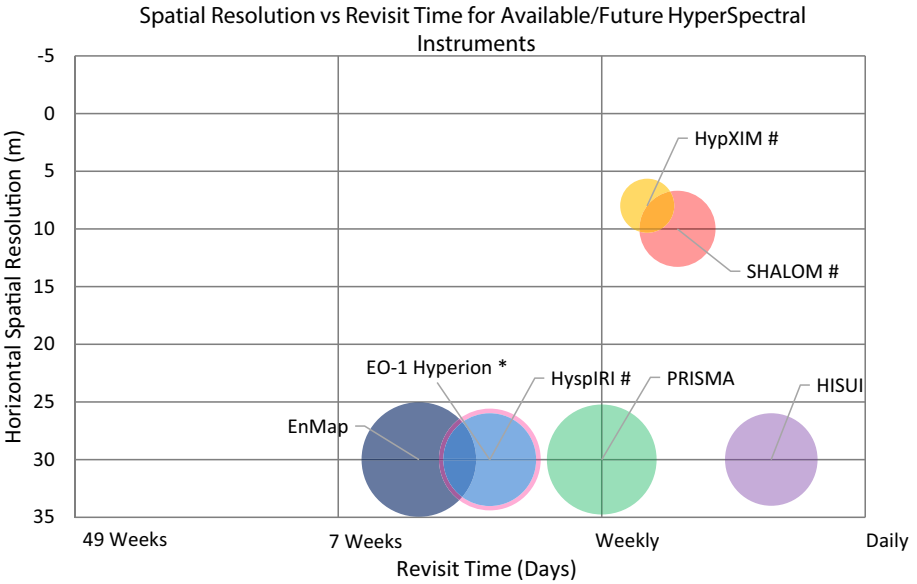

Fig. 6 Hyperspectral instrument spatial resolution and revisit time capabilities. EO-1 Hyperion was retired in 2018, while HypXIM and HyspIRI are due to launch in 2023, and SHALOM is due in 2022

shorter revisit times than the high times exhibited by current satellites. The limitations caused by high revisit times will be explored in Sect. 3.8.

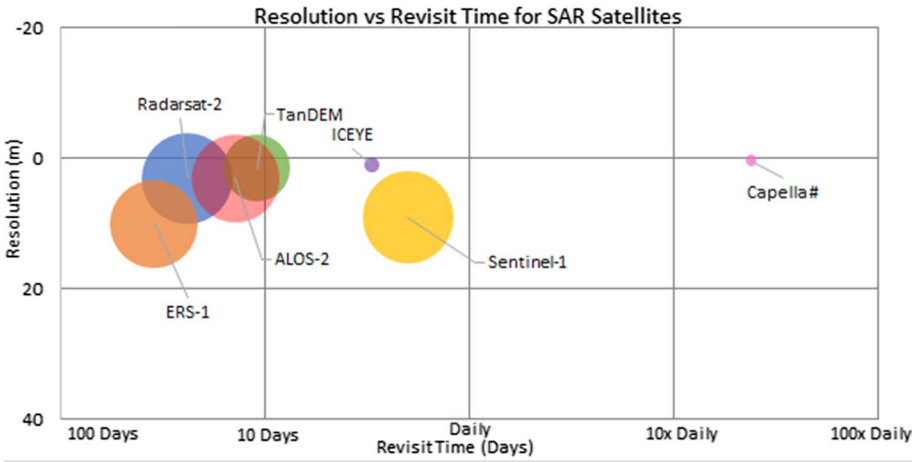

Fig. 7 Spatial resolution and revisit time capabilities of SAR satellites. Note that many have resolutions of a few metres (or less in the case of newer systems such as TanDEM and the upcoming Capella)

3 Gaps in Available Data

This section covers any fields of satellite data that are valuable to CBRN research, modelling, and monitoring but which are unexplored, or only explored to a limited degree. It also proposes possible improvements to satellite operations and data which would aid current CBRN operations.

3.1 Vertical Temperature Profile

The atmospheric temperature could affect the propagation of an agent released into the atmosphere, altering its dispersal pattern or rate. However, since the vertical temperature profiles produced by satellites start from an altitude of 45 km and continue upwards (Emery and Camps 2017), this limits the application of this data, since CBRN events occur at ground level.

If improvements could be made to allow the profiles to reach deeper into the atmosphere, then this field of data could become relevant to CBRN applications. This could be possible by utilising different wavelengths for sounding that are less absorbed by the atmosphere, or by operating at a lower orbital altitude to reduce the distances over which the attenuation of the sounding beam would occur.

3.2 Wind Velocity and Vertical Wind Profiling

With the launch of Aeolus, satellite wind velocity measurements are available at the much higher horizontal spatial resolution of 10 m compared to existing data sources such as SEVIRI and Metop which provide data on a scale of a few kilometres (Stoffelen et al. 2005) (ESA EO Directory 2020). The amount of useful data available is dependent on Aeolus' revisit time and latency. Several more similar services would need to be established to eliminate these limitations.

Aeolus data is useful for mapping wind velocity at the cloud layer and at higher altitudes, where an aerosol agent may mix with clouds or travel longer distances on the wind, but the vertical resolution of Aeolus data below 2 km is 500 m (Stoffelen et al. 2005) (ESA EO Directory 2020), meaning that satellite data on vertical wind velocity close to the ground is not detailed enough for monitoring CBRN events at ground level. This is a weakness of satellite data for CBRN monitoring purposes and for estimating the propagation of an agent. Ground-based or aerial wind speed measuring services may be more applicable for low-altitude monitoring for CBRN purposes, such as measurements taken by wind turbines and modelling predictions, such as those provided in the UK by the Numerical Objective Analysis Boundary Layer, or NOABL, which predicts of wind velocity at heights of 10, 20, and 45 m (NOABL 2020). Another example of such a service is the Global Wind Atlas, which uses microscaling on larger scale wind climate data to produce wind resource maps. Figure 8 is an example image from their website of the north of England, around Newcastle, detailing the winds at 10 m height (Global Wind Atlas 2020).

3.3 Video Footage

Video footage from space is a relatively recent development, and there are only two major services in operation: Planet's SkySat series (Planet 2020a), and Earth-i's Carbonite/Vivid-i series of satellites (ESA EO Directory 2020; Surrey Satellite Technology Ltd 2020). Between these two services, there are 17 satellites in orbit. SkySat's 15 satellites provide 90 s clips of 1080p footage at 30 frames per second and 0.8–1 m spatial resolution (Murthy et al. 2014; ESA EO Directory 2020; Planet 2020b). Each satellite has a revisit time of around 5 days, but by considering every satellite a site can be revisited multiple times per day (Planet 2020a). Carbonite's two satellites provide footage at 50 frames per second and 1 m spatial resolution for around 60 s, with a minimum of two revisits per day, with the revisit rate planned to increase as more satellites are launched (ESA EO Directory 2020). These services already provide high value data—live video of an ongoing incident would help compare models to reality when monitoring, but the small number of satellites used for this purpose limits the coverage for the immediate future.

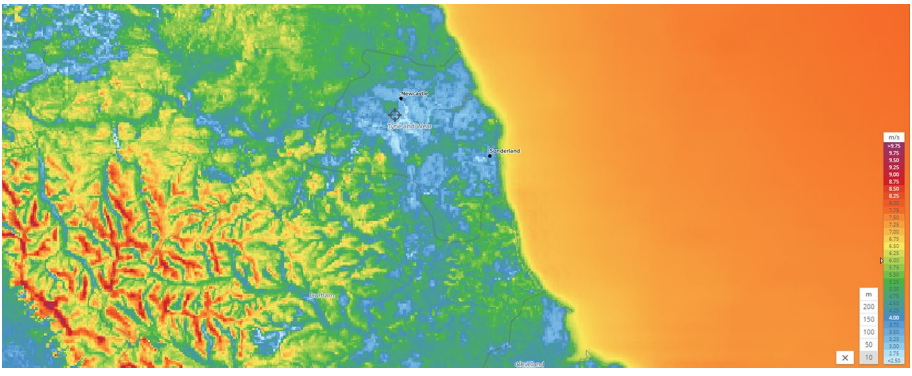

Fig. 8 A wind image from globalwindatlas.info showing generalised wind climate wind speeds for the region of the north of England around Newcastle. It is possible to zoom in further for more detail

The second issue with video for threat monitoring, which is linked very closely to the first issue with coverage, is in the length of the clips recorded. Two 60 s clips each day, as provided by the Carbonite system, may be insufficient to monitor a rapidly evolving threat event, and ideally continuous live coverage would be desirable to maximise the available situational awareness. This is not possible with the currently available satellites since the satellites pass over a target in as few as 2 min and may not revisit the target for as many as 20 days. Once the satellite constellations are expanded, however, splicing together clips from multiple imagers as they each pass over the target could provide more continuous coverage. It is not certain that Carbonite will offer this service, however, since demand for footage could be high.

3.4 Biological Detection

Unfortunately for CBRN applications, detecting biological agents from space is challenging, since many biological agents and agent releases occur on too small a scale to resolve. For example, while agents can be delivered as aerosols, a form that is detectable from space in large clouds, only the largest biological agent releases, such as the Sverdlovsk Anthrax leak of 1979, take place on a scale of kilometres and could thus be resolved by satellites (Meselson et al. 1994). Alternatively, biological agents are often disseminated through other means such as contamination of food, water, or possessions, which with the possible exception of water supply contamination (on a large scale such as rivers or reservoirs) fall outside the purview of satellite observations (Federation of American Scientists 1996).

3.5 Radiological Detection

Nuclear and radiological detection from space is largely limited by the atmosphere, which blocks almost all high-energy radiation. Additionally, the space environment has high radioactive activity of its own, including alpha, beta, and gamma rays, meaning any nuclear radiation from Earth could be obscured by cosmic radiation. The only detectable radiation would be produced either by the Cherenkov effect or by fluorescence of any emitted particles that pass through the atmosphere, both low-rate occurrences (The Royal Society 2007). This means that radiological detection from space is limited to looking for proxy indicators of the presence of radioactive material, rather than the radiation itself.

One such indicator is vegetation health. By monitoring the colouration of plants through their NDVI, Normalised Difference Vegetation Index, or another property, and with knowledge of how the properties of plants change when exposed to radiation or radioactive ions, it is possible to track the flow of contaminated groundwater around nuclear plants or material processing centres, such as waste disposal centres or weapons-grade uranium production sites, which would reveal if a leak of material has occurred, for example (UK Government 2017).

Apart from applications such as these, however, the use of satellites for nuclear monitoring purposes is largely restricted to communications and the rapid transfer of data from other monitoring devices (ESA 2008).

3.6 Chemical Detection

The resolution on most chemical detection instruments is generally too coarse for the fine level of detection needed to model CBRN events before the dispersion of the agent covers a significantly large radius. Ozone, for example, can be detected using the TROPOMI multispectral imaging spectrometer on Sentinel-5P with the finest spatial resolution being 7 by 3.5 km (Gonzalez Abad et al. 2019), and Metop detects trace gases with a spatial resolution of 12 km (Hilton et al. 2012) (ESA EO Directory 2020). These are suitable for regional detection and global mapping, but fine monitoring on a local scale requires better resolutions. Furthermore, this data is typically acquired by sounding, so the focus is on taking vertical measurements, meaning spatial resolution in the horizontal is a low priority.

One higher resolution capability of chemical detection satellites is the detection of chemical aerosols from space, which can be performed to sub-kilometre resolutions of around 250 m (Gupta and Follette-Cook 2017), sufficient to determine aerosol smoke from clouds using measurements of radiance and optical depth from an spectrometer such as MODIS or TROPOMI to determine one from the other (Gonzalez Abad et al. 2019). This is useful for CBRN purposes in kilometre-scale events, but further improvements would be valuable to monitoring metre-scale events. Taking the 2018 nerve agent poisonings in the Salisbury area as an example, the agent was delivered in liquid aerosol form via a spray from a perfume bottle (Corbin 2018). This naturally means that incidents such as this covers a scale of metres at most, beyond the limits of satellite detection.

However, simulations of the use of laser photoacoustic spectroscopy to detect chemical warfare agents suggest that a tuneable semiconductor laser could be used to match the laser transitions with the spectra of the target agents and to measure them with a high sensitivity (Patel 2008). This would require a high-power laser pointing at the Earth, which could raise concerns about safety, but this capability would nonetheless be an asset to incident detection and monitoring efforts for events involving chemical warfare agents (CWAs) or toxic industrial chemicals (TICs).

3.7 Spatial and Temporal Resolution

Spatial resolution, the smallest resolvable detail observable by an instrument, depends on the viewing distance (Selva and Krejci 2012). Satellite data is often limited in resolution because satellites observe from much farther away than other means, such as in-situ or even airborne measurements. The best commercial visual resolution available is currently 30 cm data provided by DigitalGlobe's Worldview satellite (DigitalGlobe 2020). But almost all nonvisual satellite data has a spatial resolution on the scale of kilometres or hundreds of metres, as shown in the previous sections.

The temporal resolution, or revisit time, of satellites is also an issue. Due to the nature of most satellite orbits, an imager with sufficient resolution will only pass over the target sites at certain times, so images with low latency will not always be available, since imaging a CBRN event would require being in the right place at the right time. If an incident occurs, having to wait for a satellite to pass over does not suit the urgency needed by the response. Therefore, the next section tackles latency—the time taken to get the data from command to the customer.

3.8 Latency

This subsection deals with the latency of satellite data products, including the sources of satellites' typically high delay in receiving the data after requesting it, as well as providing some examples of latency for current and future satellite data.

3.8.1 Satellite Latency Sources

Another issue with satellites and satellite data caused by their distance from the ground is the latency of the data products. The communication delay to orbit is typically higher than that of ground communications, with a direct time to orbit and back of 600 ms to Geostationary Orbit and 40 ms to (LEO) (Telesat 2018), whereas high quality cable internet typically has transfer times of 15–40 ms (George 2019), at least when communicating regionally over hundreds of km or less. Combining this with the typically large size of Earth observation data results in large transmission times.

Overall data product latency includes transmission time along with various other factors, including the coverage of both target sites and ground stations, the transmission bandwidth and speed, and the time taken to process the data into a useable product. There are also time delays associated with tasking the satellites, composed of the time taken to upload the commands followed by the wait for the satellite to pass over its target, which is dependent on the orbit's revisit time. Next comes the delay in acquiring the images and obtaining the product itself, which consists of the time taken to image the target, then waiting to reach a ground station, the time taken to download the raw data, and finally the time taken to process the raw data into products and disseminate them (Brown, Carroll and Escobar 2014; Kerr 2019). Figure 9 is a timeline diagram breaking latency down into its components.

The tasking can take up to a few days if the process has not been automated by the data supplier, and automated tasking is a recent development, and therefore is uncommon. Other factors that may affect this will include any existing relationships between clients and the supplier, since suppliers may prioritise certain customers. Also, the communication bandwidth and frequency used by the satellite may play a role. Higher frequencies have a wider bandwidth available, meaning that more data can be pushed through, increasing upload and download speeds (Rainey 2014; Nichols 2017). The time for arrival at the target can depend on the orbit. Sun-synchronous orbits, often used for Earth observation, have an endemic latency since they pass over a point on Earth at the same local time each day (ESA Enabling and Support 2020), the imagery typically being taken between 10:30 and midday for optimum lighting conditions. This not only produces a given fixed delay when waiting to reach the target or the ground station but is suboptimal for clients seeking regular coverage of a site at different times of the day.

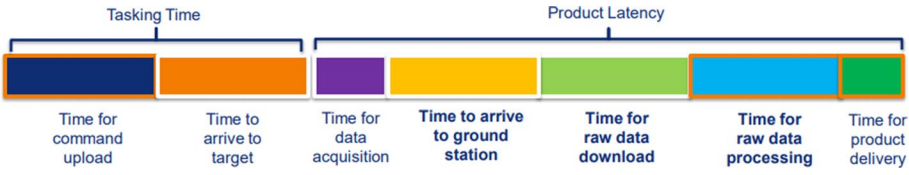

Fig. 9 Components of overall satellite latency, including tasking time and product latency. The sections are sized to give an indication of which components take the longest

In terms of the time taken for acquisition of the data, sources of latency include the number of targets required for observation, which extends waiting time if there are more targets to observe, and whether favourable weather conditions are required for observations. The latency of arrival at a ground station will depend on the same factors as arriving at a target, though an increased number of possible ground stations can reduce this. Additionally, latency can be improved by prioritising the data if the satellite is in a delay-tolerant network, in which data can be kept for several orbits before transmission (Caini 2015). Generally, delay-tolerant networks are useful for satellite data management, but they can increase the latency in obtaining the data products.

The raw data download time is dependent on download bandwidth and speed, as with the command upload time. There are more solutions in development to improve latency in this area, to be covered in Sect. 4. The ground data processing will have reduced latency as processing technology improves, using machine learning to classify and discriminate features and events of interest more rapidly.

3.8.2 Satellite Latency Examples

Featured here are three tables, Tables (1, 2, 3), containing the latencies of data products from current visual, nonvisual, and hyperspectral instruments respectively, along with their resolutions, and three more tables, Tables 4, 5 and 6, covering the same for future imaging satellites in the same domains, to give a general sense of the latencies that most satellites have, as well as an indication of how satellite data latency will change with the introduction

Table 1 Latencies for current visual imaging satellites

System	Latency	GSD
DigitalGlobe Worldview (DigitalGlobe 2020)	2–5 days	30 cm–3.7 m
Planet SkySat	2hrs	0.7 m
Elecnor Deimos-2 (ESA Copernicus 2020)	90mins	0.75–3 m
ESA Sentinels + EDRS	NRT- Hours (18 min avg.)	10/20/60 m (Sentinel 2)
Earth-i Carbonite	NRT	1 m

GSD is ground sampling distance. Note that the BlackSky and Carbonite constellations are not fully launched yet and that the Sentinels use EDRS, as in Sect. 4

Table 2 Product Latencies and ground sampling distances (GSDs) for current nonvisual satellite instruments, including SAR, spectrometers, radiometers, and lidars

System	Latency	GSD
Airbus TerraSAR-X Radar	~5 days (currently)	0.25–40 m
ESA Sentinel-5P TROPOMI	3 + hrs	7 × 3.5 km
ESA SEVIRI Surface Temp	3hrs	3 km
ESA Aeolus Wind	3hrs–30mins	3 km
EUMETSAT Metop AVHRR Wind	12hrs	4 km
ESA SEVIRI Precipitation	3hrs	5 km average

Table 3 Table of latencies and spatial resolutions for various hyperspectral imaging instruments

System/Instrument	Latency	GSD	Launch/Lifetime
NASA EO-1/Hyperion (NASA Snow and Ice Data Center 2002) (Patel 2017)	2 days	30 m	2000–2017
ISRO HySIS (ISRO 2020) (World Meteorological Organisation 2020)	< 12hrs	30 m	2018-
ASI PRISMA (ESA EO Directory 2020)	< 14 days	30 m	2019-
ESA PROBA (ESA Earth Online 2020)	24hrs	17-34 m	2001-
ISS/HISUI (Matsunaga et al. 2018)	Near-real-time*	20 m	2019-

Also included is one recent historical instrument, EO-1′s Hyperion. Note that HISUI on the ISS only transmits a portion of its data with near-real-time latency, the rest is stored and manually delivered on return missions from the International Space Station (ISS)

Table 4 Information for upcoming visual imaging satellites, including launch years

System/Instrument	Latency	GSD	Launch year
ISRO CartoSat 3 Series	Requested	0.25–13.5 m	2020
LandSat 9	3 days–4 h	15 m	2020
BlackSky constellation (full)	90 min	1 m	> 2021 (16 sats)
ESA/JAXA EarthCARE Visible	5.1 h	500 m	2022

Table 5 Latency and resolution information for upcoming nonvisual imagers, such as radars and sounders

Future nonvisual	Latency	GSD	Launch year
ESA/JAXA EarthCARE Radar	5.1 h	750 m	2022
NASA JPSS-2	87 min	> 375 m	2021
ISRO RISAT-2A (Dadhwal 2013)	Requested	0.25 m	2020
ESA FLEX	24 h	< 300 m	2020
ESA Sentinel 4/5	< 30 min (EDRS)	8 km	2021

Table 6 Predicted latency values and spatial resolutions for future hyperspectral imaging instruments, along with launch years

System/Instrument	Latency	GSD	Launch year
CNES HypXIM (Michel, Gamet and Lefevre-Fonollosa 2011) (Menz et al. 2016)	< 3 days	8–100 m	2023
ASI/ISA SHALOM (Feingersh and Dor 2015)	< 7 days	10 m	2022
DLR EnMap HSI (ESA EO Directory 2020)	< 2.5 days	30 m	2020
NASA HyspIRI (Lee et al. 2015)	NRT (Mandl 2010)	30–60 m	2023

HyspIRI is experimenting with a multiground station concept for low latency, while the others will likely rely on traditional methods

of emergent technologies described in Sect. 4. NRT stands for Near-Real-Time, and the GSD, or Ground Sampling Distance, is another term for spatial resolution.

What these tables show is that only satellites utilising emergent technologies, to be discussed in Sect. 4, have the capability for latencies on the scale of minutes rather than hours. This technology will be necessary in order to match urgency requirements for CBRN monitoring.

4 Emergent Technologies

There are several developing technologies and methods that will lead to significant improvements to latency and resolution including new instruments, new platforms at different altitudes, constellations, optical data transmission, and improved onboard processing.

4.1 Synthetic Aperture Radar and Lidar

Synthetic Aperture Radars have the advantages of radar such as night-time imaging and working through cloud cover, but with higher resolution, sub-metre in the case of the TerraSAR-X instrument (Fritz and Eidener 2013).

Laboratory tests have been conducted with infrared synthetic aperture lidars suggesting that a synthetic aperture lidar could produce images with a resolution of less than a metre and sub-millimetre modelling precision (Terroux et al. 2017), a vast improvement over current spaceborne lidar instruments, which provide resolutions of around 25 m, such as the GEDI instrument on the ISS (World Meteorological Organisation 2020).

4.2 Very Low Earth Orbit (VLEO)

By developing satellites for use in Very Low Earth Orbits (VLEO), which are orbits with an altitude of 450 km or lower (Virgili-Llop et al. 2014) (Dakka 2018), the spatial resolution and link budget can be improved by increasing proximity to the imaging target. At these low altitudes, the atmosphere is sufficient to produce significant drag on the spacecraft (Virgili-Llop et al. 2014) (Dakka 2018), which then needs to perform drag compensation with chemical or electric propulsion (Dakka 2018). Furthermore, the atmospheric presence at these altitudes causes erosion of spacecraft outer surfaces with atomic oxygen found in the upper atmosphere, so a countermeasure would need to be implemented (Banks, De Groh and Miller 2004; Samwel 2014). Figure 10 depicts a design for a VLEO satellite along with some of the advantages and disadvantages of the system. The design originates from Thales Alenia Space, who have conducted significant previous research into VLEO satellites (Walsh and Berthoud 2016, 2017; Bacon and Olivier 2017).

4.3 High-Altitude Pseudo-Satellites

With many of the benefits of the use of VLEO, there are various high-altitude platforms either available or in development. These are not truly satellites, since they operate at altitudes of around 20 km, and they take the form of unmanned airships, planes or gliders (Gonzalo et al. 2018). These platforms are primarily aimed at surveillance or providing

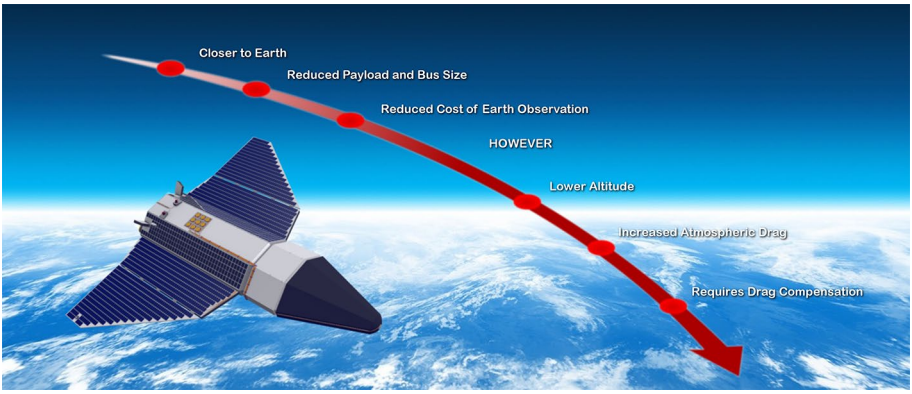

Fig. 10 A design example of a VLEO satellite, and a trade-off associated with the use of such a platform. VLEO satellites will likely be cheaper to use in addition to improved resolution and latency, at the cost of the extra design challenges needed to implement them. *Image Credit*: Thales Alenia Space

5G internet networks, but they also have potential applications for low-latency Earth observation.

One notable example is Airbus' Zephyr high-altitude UAV, four of which have been built and three of which are in use by the UK government (Airbus 2020b; UK Government 2016). Zephyr typically operates at a maximum altitude of around 21 km (Airbus 2020b). Another example is Thales' StratoBus, a high-altitude solar airship intended for use at 20 km with a 250 kg payload (Thales Group 2017). It is expected to be capable of five-year missions with annual servicing, and a prototype is planned for late 2020 with a market release in 2021 (Thales Group 2017). Figure 11 is an image from Thales Alenia Space depicting StratoBus.

A disadvantage of these platforms due to their proximity to the ground is that they will image a smaller area, and will not have the coverage of satellites, but this is counterbalanced by the long staying time and the improved resolution and latency.

4.4 Constellations

Another new development in satellite technology is the use of satellite constellations (Thales Group 2019). The global coverage provided by constellations has the effect of improving the revisit time and latency, since at least one of the satellites in the constellation will likely have a view of the target area at any given point. This eliminates one of the biggest problems with satellites for CBRN applications, which is that coverage of an incident while it is occurring could not be guaranteed.

Several constellations of varying sizes are already in the process of launching their first satellites, such as BlackSky, Planet's SkySat and Carbonite. BlackSky is a constellation of 60 satellites developed by SpaceFlight Industries and Thales Alenia Space, with 2 currently in orbit, which when complete will produce 1 m spatial resolution global images every 90 min (ESA EO Directory 2020). SkySat and Carbonite will image and record video at 1 m or finer spatial resolution, as described in Sect. 3.3 (ESA EO Directory 2020). The first

Fig. 11 A depiction of the StratoBus High-Altitude Pseudo-Satellite being developed by Thales Alenia Space for market release in 2021

BlackSky satellites are already producing images, such as Fig. 12, an image of Melbourne taken in March 2019 (BlackSky 2019).

4.5 Optical Laser Data Transmission

The concept of utilising optical lasers to transmit data between satellites at a high rate can be used to reduce latency. By having imaging Low Earth Orbit satellites first transfer their data to a Geostationary satellite over a ground station, and then transmitting the data from that geostationary satellite to the ground, the latency in waiting for the imager to reach a ground station is eliminated (ESA EO Directory 2020; Airbus 2020a; Airbus 2019), resulting in extremely low data download times and minimal product latency.

Airbus is already providing this service to the four Sentinel satellites using the European Data Relay System, or EDRS, with latencies ranging from near-real-time to a few hours, averaging at 18 min (Airbus 2020a) (Copernicus Space Component Mission Management Team 2019). Two EDRS satellites, EDRS-A and C are in orbit currently, with a third due to launch in 2024 (Airbus 2019). This service is available commercially, with price negotiable. The concept at use in EDRS is demonstrated in Fig. 13, an image from Airbus and ESA depicting the satellites relaying data.

4.6 Onboard Processing

An alternative technology and methodology for reducing satellite data latency is the use of onboard processing to process the raw data into the products before they reach the ground (Kerr 2019; Kerr et al. 2018). This eliminates time spent waiting for the data to be processed after transmission to the ground station, and typically the processed data products

Fig. 12 An image of Melbourne in the last week of March 2019 acquired by BlackSky's first two satellites. Subsequent images of the same area from the satellites during that week demonstrate the imagers' resolution capabilities by showing the motion of traffic along the roads

are smaller in terms of file size compared to the raw data, meaning that downlink times will additionally be shorter (Kerr 2019).

A Horizon 2020 research programme called 'EO-Alert' is working with the Deimos-2 and TerraSAR-X satellite operators to develop improved onboard processing technology.

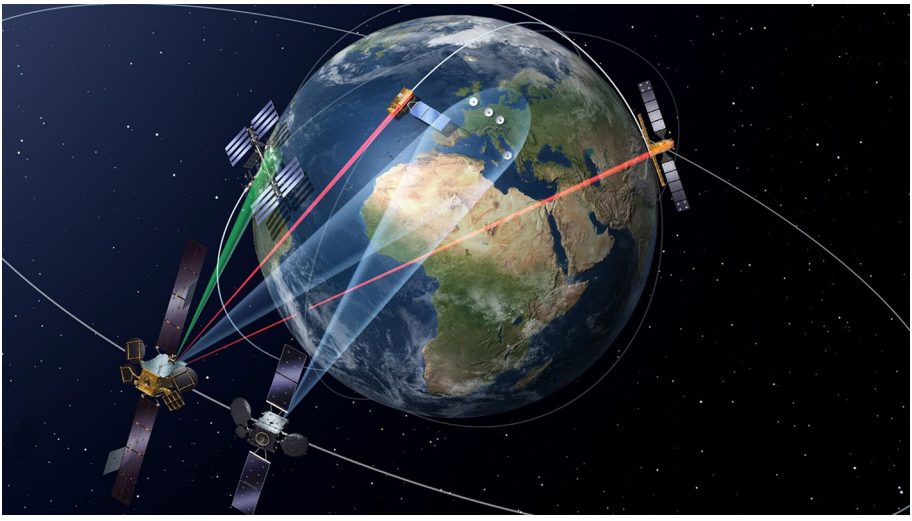

Fig. 13 A depiction of data being relayed from satellite to satellite in the European Data Relay System (EDRS)

They are initially focused on improving the latency for Deimos-2′s optical data and TerraSAR-X's radar data, to improve latency for extreme weather, convective storms and surface high winds for ship location monitoring (Kerr 2019; Kerr et al. 2018).

The aim of the project is to reduce customer waiting times to under half an hour, with a one-hour advance request for data required (Kerr et al. 2018). This 30 min latency is comparable to that provided by the EDRS optical transmission system (Copernicus Space Component Mission Management Team 2019), though there is one potential issue with data pre-processing before transmission: while many companies and industries require the processed data products for their applications, academic researchers often make use of the raw data. This produces a requirement to store and send both the raw data and the data products that have been processed onboard. The system designed by EO-Alert has two separate channels for acquired data, one of which processes the data into products, and the other of which stores the raw data (Kerr 2019). This new chain alters the communication unit to be capable of transmit processed products as well as raw data, with an alternative path after data acquisition in which a copy of the raw data is processed on board the satellite. This processed data is then compressed in the same fashion as the raw data is, and the two are transmitted to the ground station in separate streams, a high-volume stream of raw data and a low-volume stream of processed images (Kerr et al. 2018).

5 Upcoming Missions and Instruments

Satellite missions in subsequent years may provide new data with improved resolution, revisit times, latency, or explore new fields for satellite earth observation utilising instruments and technologies such as those in Sect. 4. This section covers particularly notable examples of interest to CBRN monitoring, though it is by no means an exhaustive list.

5.1 LandSat 9: Imagery

Launching in December 2020 is the next satellite in NASA's Landsat series (Rocket-Launch.live 2020). Landsat 9 is mostly an updated replication of its predecessor, with some extra additions (NASA 2020b). It will carry two instruments, the Operation Land Imager 2 (OLI-2) and the Thermal Infrared Sensor 2 (TIRS-2). It will provide images in the optical at 30 m, at 15 m in the panchromatic, and of 100 m resolution in thermal infrared. The image swath will be 185 km wide, producing global coverage every 16 days (NASA 2020a). The resolution on these images may be insufficient for CBRN models, except for the panchromatic, but the addition of another satellite alongside Landsat 8 will improve coverage.

5.2 JPSS-2: Atmospheric, Chemical, and Radiation Budget Monitoring

The second satellite in NASA's Joint Polar Satellite System, or JPSS, is due to launch in 2021. It will carry five instruments: ATMS, the Advanced Technology Microwave Sounder; CrIS, the Cross-track Infrared Sounder; OMPS, the Ozone Mapping and Profile Suite; VIIRS, the Visible/Infrared Imager Radiometer Suite; and RBI, the Radiation Budget Instrument (World Meteorological Organisation 2020).

ATMS sounds for temperature, humidity, and precipitation mapping with a spatial resolution between 16 and 75 km depending on the imaging channels (World

Meteorological Organisation 2020). CrIS also sounds for temperature and humidity, along with coarse Ozone profile and column mapping of greenhouse gases. It does these in 3-by-3 14 km grids totalling up to 48 km in size, with an average sampling distance of 16 km (World Meteorological Organisation 2020). OMPS is a prism spectrometer for mapping stratospheric chemistry, recording the mole fractions of several chemicals such as BrO, ClO, SO_2, NO_2, and several others, with a resolution of 300 km horizontally and 2.2 km vertically (World Meteorological Organisation 2020). VIIRS will produce visible/infrared radiometry images for purposes of monitoring biomass and cloud properties with a resolution between 375 and 750 m depending on the channels (World Meteorological Organisation 2020), and RBI maps the radiation budget across the earth with 30 km resolution in three channels, for total, short wave, and long wave, respectively (World Meteorological Organisation 2020). All of these instruments achieve global coverage twice a day except for OMPS, which produces global data every 4 days.

The resolution of these data products is very coarse compared to requirements for CBRN modelling purposes, but JPSS-2 nevertheless is a versatile satellite that provides data on a wide range of topics relevant to chemical monitoring, and could have applications to larger scale events should they occur.

5.3 EVI-4 EMIT: Analysis of Dust Aerosols

Another upcoming NASA instrument of interest for CBRN applications is EMIT, the Earth surface Mineral dust source InvesTigation, an instrument to be deployed on intended to be flown on the international space station in 2022 (JPL Artificial Intelligence Group 2019; Yelamanchili et al. 2019) (NASA 2019). It is a hyperspectral instrument intended to determine the mineral composition of dust aerosol sources and investigate the effects of the dust aerosols on atmospheric temperature (NASA 2019) (Yelamanchili et al. 2019). EMIT is intended for use investigation of natural dust aerosol sources, but it is certainly possible that this technology could be applied to artificial aerosol sources in a CBRN scenario. Not much information on the specifications of EMIT is currently available, but the mission demonstrates the sorts of instruments that could be developed for the field in the future, since source estimation is a priority in CBRN scenario modelling.

5.4 Ingenio: Terrain Mapping

SEOSat Ingenio is Spain's first optical imaging satellite, was launched in November 2020, but the rocket failed. The primary manufacturer and operator of the spacecraft is Airbus Defence and Space Spain, with some parts produced by Thales Alenia Space (ESA EO Directory 2020). It carries three instruments: A multispectral imager, a panchromatic imager, and an ultraviolet and visible atmospheric sounder. The images will have a resolution of 10 m in the multispectral, 2.5 m in the panchromatic, and the atmospheric sounder will have a resolution of 10 km at the sub-satellite point, tracking a wide range of atmospheric chemicals similar to those monitored by JPSS-2(ESA EO Directory 2020).

Ingenio will join the wide range of optical imaging satellites available, A resolution Ingenio satellite could join the wide either comparable to or improved over many of the

other options, so data from this satellite could prove useful for improving the fidelity of visual terrain mapping for CBRN models.

5.5 DarkCarb: Thermal Imaging

DarkCarb is a design for a thermal imager in development by Surrey Satellite Technology, or SSTL (Surrey Satellite Technology Ltd 2019). The objective is to provide a thermal video imaging capability for the Carbonite satellite constellation, aimed at applications including industrial monitoring, disaster response support, including fires and volcanoes, environmental monitoring such as the mapping of urban heat islands, and the monitoring of large ships and other vehicles for defence purposes (Surrey Satellite Technology Ltd 2019).

The instrument promises a ground sampling distance or spatial resolution of 3.5 m, with the capability to record 60 s video clips at 1–25 fps, distinguishing temperature differences as small as 2 K (Surrey Satellite Technology Ltd 2019). Several of the intended applications are relevant to CBRN incident monitoring, including heat island monitoring and the various disaster response capabilities, and the resolution is potentially enough for monitoring urban-scale events.

6 Conclusions

There is a wide range of satellite data available that can be used to support CBRN incident monitoring and modelling applications, by providing images and other data. However, much of the data has coarse spatial resolution and long revisit times. CBRN incidents require urgent data for situational awareness, although archive data can be used for modelling and training, and several of these limitations become less significant when using satellite data in pre-planning for incident mitigation, or for long-term remediation and monitoring after an incident has occurred.

While most individual satellites in the immediate future do not offer great improvements in resolution, there are many technologies in development that promise major improvements to latency, coverage, and in some cases resolution. These include High-Altitude Pseudo-Satellites and Very Low Earth Orbit satellites, along with constellations. Additionally, systems such as the EDRS optical data transmission system and EO-Alert's onboard processing system will help reduce the latency of satellite data. These improvements to latency and coverage will mitigate the limited footprint size of high-resolution satellite imaging, while the resolution improvements will allow incidents that were previously undetectable to be spotted and will bring various fields of satellite data new relevance to CBRN modelling and monitoring applications. New and novel instruments and detectors are being aimed at the gaps in available CBRN data from satellites, such as the detection of a wider range of chemicals and new parameters useful to incident monitoring, such as the source estimation capabilities to be provided by EMIT. These improvements will mean that satellite data will become even more useful to the field of CBRN over the next decade.

Acknowledgements This research was partially funded by the European Space Agency EUROSIM CBRN contract, led by Riskaware Ltd, and the authors are grateful for the guidance and support from both of these organisations.

Authors' Contributions Gary Sutlieff was the lead author, Prof. Lucy Berthoud contributed to editing and acted in a supervisory capacity, and Mark Stinchcombe conducted the preliminary work at Thales Alenia Space that led to this work.

Funding Funding for this research was supplied by the EPSRC iCASE studentship no. 19000187 supported by Thales Alenia Space UK, or TAS UK, as well as by ESA contract 4000128582/19/uk/AB EUROSIM CBRN.

Availability of Data and Material All the data (resolutions of various satellites, etc.) was collected freely online and will therefore be available at the sources given.

Code Availability No custom code was used in the creation of this paper.

Declarations

Conflict of interest There are no known conflicts of interest involved with this research.

References

Airbus (2019) Successful launch of the second SpaceDataHighway satellite on Ariane 5 - Space - Airbus. Available at: https://www.airbus.com/newsroom/press-releases/en/2019/08/successful-launch-of-the-second-spacedatahighway-satellite-on-ariane-5.html (Accessed: 4 March 2020).

Airbus (2020a) SpaceDataHighway-Telecommunications - Airbus. Available at: https://www.airbus.com/space/telecommunications-satellites/space-data-highway.html (Accessed: 4 March 2020).

Airbus (2020b) Zephyr-UAV-Airbus, Airbus. Available at: https://www.airbus.com/defence/uav/zephyr.html (Accessed: 18 February 2020).

Bacon, A. and Olivier, B. (2017) Skimsats: bringing down the cost of Earth Observation, In: Proceedings of the 12th reinventing space conference. Springer International Publishing, pp. 1–7. https://doi.org/10.1007/978-3-319-34024-1_1.

Banks, B. A., De Groh, K. K. and Miller, S. K. (2004) Low earth orbital atomic oxygen interactions with spacecraft materials. Available at: http://www.sti.nasa.gov (Accessed: 18 December 2019).

BlackSky (2019) First look at imagery from global-1 and -2-Black Sky. Available at: https://www.blacksky.com/2019/04/09/first-look-at-imagery-from-global-1-and-2/ (Accessed: 6 March 2020).

Bluefield (2020a) Bluefield | Precise and scalable methane monitoring via AI applied to satellite imagery. Available at: https://bluefield.co/#technology (Accessed: 6 March 2020).

Bluefield (2020b) Bluefield detects large methane release in Florida | Bluefield. Available at: https://bluefield.co/press-release-florida-methane-0720/ (Accessed: 12 November 2020).

Borde R, Hautecoeur O, Carranza M (2016) EUMETSAT global AVHRR wind product. J Atmos Ocean Technol 33(3):429–438. https://doi.org/10.1175/JTECH-D-15-0155.1

Brown ME, Carroll ML, Escobar VM (2014) User needs and assessing the impact of low latency NASA Earth observation data availability on societal benefit. Space Policy 30:135–137. https://doi.org/10.1016/j.spacepol.2014.05.002

Caini, C. (2015) Delay-tolerant networks (DTNs) for satellite communications. In: Advances in delay-tolerant networks (DTNs). Elsevier, pp. 25–47. https://doi.org/10.1533/9780857098467.1.25.

Carlsen L (2018) After salisbury nerve agents revisited. Mol Inform 38(8–9):1800106. https://doi.org/10.1002/minf.201800106

Centre for strategy & evaluation services (2011) Ex-post evaluation of PASR activities in the field of security and interim evaluation of FP7 security research CBRN case study. Available at: www.cses.co.uk (Accessed: 13 November 2019).

Copernicus space component mission management team (2019) Sentinel high level operations plan (HLOP). Available at: https://sentinel.esa.int/web/sentinel/user-guides/sentinel-1-sar/document-library/-/asset_publisher/1dO7RF5fJMbd/content/sentinel-high-level-operations-plan#:~:text=The sentinel high level operations,of sentinels and sentinel facilities. (Accessed: 4 March 2020).

Corbin, J. (2018) Skripal poisoning: policeman's family 'lost everything' because of novichok - BBC news, BBC news. Available at: https://www.bbc.co.uk/news/uk-46290989 (Accessed: 13 December 2019).

Dadhwal, V. K. (2013) 50 th Session of scientific & technical subcommittee of COPUOS. Available at: https://www.unoosa.org/oosa/en/ourwork/copuos/stsc/2013/index.html (Accessed: 6 April 2020).

Dakka, S. M. (2018) VLEO satellites- a new earth observation space systems commercial and business model. In: IET Conference publications. Institution of Engineering and Technology. https://doi.org/10.1049/cp.2018.1718

DigitalGlobe (2020) Specifications deliverables. Available at: www.digitalglobe.com (Accessed: 4 March 2020).

Emery, W. and Camps, A. (2017) Chapter 8-Atmosphere applications, introduction to satellite remote sensing. https://doi.org/10.1016/B978-0-12-809254-5.00008-7.

ESA (2008) ESA - ESA satellite technology enhances nuclear monitoring. Available at: https://www.esa.int/Applications/Telecommunications_Integrated_Applications/ESA_satellite_technology_enhances_nuclear_monitoring (Accessed: 13 December 2019).

ESA (2018) ESA-Aeolus wows with first wind data. Available at: https://www.esa.int/Applications/Observing_the_Earth/Aeolus/Aeolus_wows_with_first_wind_data (Accessed: 6 March 2020).

ESA Copernicus (2020) *DEIMOS-2*. Available at: https://spacedata.copernicus.eu/web/cscda/missions/deimos-2 (Accessed: 6 March 2020).

ESA Earth Online (2020) Proba CHRIS level 1A-view data product-Earth online-ESA. Available at: https://earth.esa.int/web/guest/-/proba-chris-level-1a-1488 (Accessed: 6 March 2020).

ESA Enabling and Support (2020) Types of orbits. Available at: https://www.esa.int/Enabling_Support/Space_Transportation/Types_of_orbits (Accessed: 4 March 2020).

ESA EO Directory (2020) ESA eoPortal satellite missions directory. Available at: https://directory.eoportal.org/web/eoportal/satellite-missions/a (Accessed: 3 November 2020).

EUMETSAT (2020a) Current satellites. Available at: https://www.eumetsat.int/website/home/Satellites/CurrentSatellites/index.html (Accessed: 4 November 2020).

EUMETSAT (2020b) EUMETSAT Product navigator. Available at: https://navigator.eumetsat.int/start (Accessed: 4 November 2020).

EUMETSAT CM SAF (2020) CM SAF Web User Interface // Product // Home. Available at: https://wui.cmsaf.eu/safira/action/viewProduktHome?menuName=PRODUKT_HOME (Accessed: 22 January 2020).

EUMETSAT H-SAF (2020) H-SAFOfficial web site. Available at: http://hsaf.meteoam.it/ (Accessed: 22 January 2020).

EUMETSAT LSA SAF (2020) EUMETSAT LSA SAF Homepage. Available at: https://landsaf.ipma.pt/en/ (Accessed: 3 November 2020).

Federation of American Scientists (1996) *US* Army field manual 8–9 Part II/Chptr 1 introduction, army field manual 8–9. Available at: https://fas.org/nuke/guide/usa/doctrine/dod/fm8-9/2ch1.htm (Accessed: 11 December 2019).

Feingersh T, Dor EB (2015) SHALOM-A commercial hyperspectral space mission. In: Qian S-E (ed) Optical payloads for space missions. John Wiley, Chichester, UK, pp 247–263. https://doi.org/10.1002/9781118945179.ch11

Freitas SC et al (2010) Quantifying the uncertainty of land surface temperature retrievals from SEVIRI/Meteosat. IEEE Trans Geosci Remote Sens 48(1):523–534. https://doi.org/10.1109/TGRS.2009.2027697

Fritz, T. and Eidener, M. (2013) TerraSAR-X Ground segment-basic product specification document. Available at: https://sss.terrasar-x.dlr.de/docs/TX-GS-DD-3302.pdf.

George, N. (2019) *What Internet Speed Do I Need? | FAQs On Internet Speeds*, *allconnect.com*. Available at: https://www.allconnect.com/blog/faqs-internet-speeds-what-speed-do-you-need (Accessed: 4 March 2020).

Global Wind Atlas (2020) Global wind atlas. Available at: https://globalwindatlas.info/ (Accessed: 6 March 2020).

Gonzalez Abad G et al (2019) Five decades observing Earth's atmospheric trace gases using ultraviolet and visible backscatter solar radiation from space. J Quant Spectrosc Radiat Transf. https://doi.org/10.1016/j.jqsrt.2019.04.030

Gonzalo J et al (2018) On the capabilities and limitations of high altitude pseudo-satellites. Prog Aerosp Sci. https://doi.org/10.1016/j.paerosci.2018.03.006

Göttsche FM et al (2016) Long term validation of land surface temperature retrieved from MSG/SEVIRI with continuous in-situ measurements in Africa. Remote Sens MDPI AG. https://doi.org/10.3390/rs8050410

Gupta, P. and Follette-Cook, M. (2017) Aerosol observations from satellites: brief theory & existing products. Available at: www.nasa.gov (Accessed: 4 March 2020).

Hilton F et al (2012) Hyperspectral earth observation from IASI. Bull Am Meteor Soc 93(3):347–370. https://doi.org/10.1175/BAMS-D-11-00027.1

Houses of Parliament (2019) POSTNOTE 596 March 2019 - Chemical Weapons. Available at: www.parliament.uk/post (Accessed: 6 December 2019).

ISRO (2020) ISRO Develops Optical Imaging Detector Array for Hyperspectral Imaging Applications-ISRO. Available at: https://www.isro.gov.in/isro-develops-optical-imaging-detector-array-hyperspectral-imaging-applications (Accessed: 6 March 2020).

Joint Emergency Services Interoperability Programme (JESIP) (2016) Responding to a CBRN(e) event: joint operating principles for the emergency services. Available at: https://www.gov.uk/government/publications/counter-terrorism-strategy-contest (Accessed: 13 November 2019).

JPL (2020) GHRSST Level 2P Atlantic regional skin sea surface temperature from the spinning enhanced visible and infrared imager (SEVIRI) on the meteosat second generation (MSG-3) satellite (GDS version 2) | PO.DAAC. Available at: https://podaac.jpl.nasa.gov/dataset/MSG03-OSPO-L2P-v1.0 (Accessed: 15 January 2020).

JPL Artificial Intelligence Group (2019) EMIT. Available at: https://ai.jpl.nasa.gov/public/projects/emit/ (Accessed: 28 February 2020).

Kerr, M. *et al.* (2018) EO-ALERT: Next generation satellite processing chain for rapid civil alerts, conference: 6th international workshop on on-board payload data compression-OBPDC. Available at: https://www.researchgate.net/publication/329308599_EO-ALERT_Next_Generation_Satellite_Processing_Chain_for_Rapid_Civil_Alerts (Accessed: 19 November 2020).

Kerr, M. (2019) Novel satellite architectures for very low latency eo data products that meet societal needs. Available at: https://www.unoosa.org/documents/pdf/psa/activities/2019/UNAustria2019/KerrSatelliteArchitecture.pdf (Accessed: 4 March 2020).

Lee CM et al (2015) An introduction to the NASA hyperspectral infrared imager (HyspIRI) mission and preparatory activities. Remote Sens Environ 167:6–19. https://doi.org/10.1016/j.rse.2015.06.012

Mandl, D. (2010) HyspIRI Low Latency Concept & Benchmarks. Available at: https://ntrs.nasa.gov/search.jsp?R=20100032939 (Accessed: 6 March 2020).

Matsunaga, T. et al. (2018) HISUI Status toward FY2019 launch and collaboration with other missions. Available at: https://hyspiri.jpl.nasa.gov/downloads/2018_Workshop/day3/14_1808_HISUI_Matsunaga_04b.pdf (Accessed: 6 March 2020).

Menz, G. *et al.* (2016) European association of remote sensing laboratories 36 th EARSeL symposium 'frontiers in earth observation'. Available at: http://www.earsel.org/symposia/2016-symposium-Bonn/ (Accessed: 27 March 2020).

Meselson M et al (1994) The sverdlovsk anthrax outbreak of 1979. Science. https://doi.org/10.1126/science.7973702

Michel, S., Gamet, P. and Lefevre-Fonollosa, M. J. (2011) HYPXIM A hyperspectral satellite defined for science, security and defence users, Workshop on hyperspectral image and signal processing, evolution in remote sensing, (June). https://doi.org/10.1109/WHISPERS.2011.6080864.

Murthy, K. et al. (2014) 'SkySat-1: very high-resolution imagery from a small satellite. In: Sensors, systems, and next-generation satellitesXVIII. SPIE, p. 92411E. https://doi.org/10.1117/12.2074163.

NASA (2016) Imaging a Methane Leak from Space. Available at: https://visibleearth.nasa.gov/images/88245/imaging-a-methane-leak-from-space (Accessed: 6 March 2020).

NASA (2019) Earth surface mineral dust source investigation *(EVI-4)* | NASA's Earth observing system. Available at: https://eospso.nasa.gov/missions/earth-surface-mineral-dust-source-investigation-evi-4 (Accessed: 6 March 2020).

NASA (2020a) Instruments « Landsat Science. Available at: https://landsat.gsfc.nasa.gov/landsat-9/instruments/#tirs (Accessed: 4 March 2020).
NASA (2020b) Landsat 9 Overview « Landsat Science. Available at: https://landsat.gsfc.nasa.gov/landsat-9/landsat-9-overview/ (Accessed: 4 March 2020).
Nichols, S. (2017) L/Ku/Ka-band satellites–what does it all mean?, getconnected.aero. Available at: https://www.getconnected.aero/2017/09/lkuka-band-satellites-mean/ (Accessed: 4 March 2020).
NOAA Office of Satellite and Product Operations (2017) Sounding products. Available at: https://www.ospo.noaa.gov/Products/atmosphere/soundings/index.html (Accessed: 3 March 2020).
NOABL (2020) UK Wind speed database program-the NOABL database with postcode converter. Available at: http://www.wind-power-program.com/UK_wind_speed_database.htm (Accessed: 3 March 2020).
NOAA OSPO (2014) What is a Sounding. Available at: https://www.ospo.noaa.gov/Products/atmosphere/soundings/wsounding.html (Accessed: 3 March 2020).
Patel CKN (2008) Laser photoacoustic spectroscopy helps fight terrorism: high sensitivity detection of chemical warfare agent and explosives. Eur Phys J Spec Top 153:1. https://doi.org/10.1140/EPJST/E2008-00383-X
Patel, K. (2017) A Farewell to EO-1: Celebrating 17 Years of NASA's 'Little Earth Satellite That Could' « Landsat Science, NASA LandSat Science. Available at: https://landsat.gsfc.nasa.gov/a-farewell-to-eo-1-celebrating-17-years-of-nasas-little-earth-satellite-that-could/ (Accessed: 27 March 2020).
Planet (2020a) *Satellite Imagery Tasking*. Available at: https://www.planet.com/products/hi-res-monitoring/ (Accessed: 4 March 2020).
Planet (2020b) SkySat Imagery Product Specification. Available at: https://assets.planet.com/docs/Planet_SkySat_Imagery_Product_Specification_Jan2020.pdf (Accessed: 4 March 2020).
Pumphrey HC et al (2018) MLS measurements of stratospheric hydrogen cyanide during the 2015–2016 El Niño event. Atmos Chem Phys Copernic GmbH 18(2):691–703. https://doi.org/10.5194/acp-18-691-2018
Rainey, K. (2014) Ka-Band Represents the Future of Space Communications. Available at: https://www.nasa.gov/mission_pages/station/research/news/ka_band (Accessed: 4 March 2020).
Ramírez- Beltrán ND et al (2019) A satellite algorithm for estimating relative humidity, based on GOES and MODIS satellite data. Int J Remote Sens 40(24):9237–9259. https://doi.org/10.1080/01431161.2019.1629715
Reitebuch, O. (2008) The Wind Lidar Mission ADM-Aeolus Recent Science Activities and Status of Instrument Development. Available at: http://www.pa.op.dlr.de/aeolus/Campaigns_Pub/Reitebuch1_ADM_Feb08.pdf (Accessed: 15 January 2020).
RocketLaunch.live (2020) Launch Schedule [Earth Observation Satellite]-RocketLaunch.Live. Available at: https://www.rocketlaunch.live/?tag=earth-observation-satellite (Accessed: 4 March 2020).
Samwel SW (2014) Low earth orbital atomic oxygen erosion effect on spacecraft materials. Space Res J 7(1):1–13. https://doi.org/10.3923/srj.2014.1.13
Schmid, J. (2000) The SEVIRI Instrument. Available at: https://www.researchgate.net/publication/228530470_The_SEVIRI_instrument (Accessed: 14 January 2020).
Selva D, Krejci D (2012) A survey and assessment of the capabilities of cubesats for Earth observation. Acta Astronautica. https://doi.org/10.1016/j.actaastro.2011.12.014
Stoffelen A et al (2005) The atmospheric dynamics mission for global wind field measurement. Bull Am Meteor Soc 86(1):73–87. https://doi.org/10.1175/BAMS-86-1-73
Straume, A. G. et al. (2017) The ESA ADM-Aeolus Doppler Wind Lidar Mission-Status and validation strategy ECMWF/ESA Workshop: Tropical modelling, observations and assimilation. Available at: http://www.esa.int/esaLP/LPadmaeolus.html (Accessed: 15 January 2020).
Surrey Satellite Technology Ltd (2019) *Doing space diferently*, *SSTL Page*. Available at: https://www.sstl.co.uk/ (Accessed: 29 February 2020).
Surrey Satellite Technology Ltd (2020) SSTL's Space Portfolio - CARBONITE-2 | SSTL. Available at: https://www.sstl.co.uk/space-portfolio/launched-missions/2010-2020/carbonite-2-launched-2018 (Accessed: 9 January 2020).
Telesat (2018) Real-Time latency rethink possibilities with remote networks. Available at: https://www.telesat.com/wp-content/uploads/2020/07/Real-Time-Latency-Rethinking-Remote-Networks.pdf (Accessed: 4 March 2020).
Terroux, M. *et al.* (2017) Synthetic aperture lidar as a future tool for earth observation. In: SPIE-Intl Soc Optical Eng, p. 196. https://doi.org/10.1117/12.2304256.
Thales Group (2017) What's up with Stratobus*?* Available at: https://www.thalesgroup.com/en/worldwide/space/news/whats-stratobus (Accessed: 4 March 2020).

Thales Group (2019) Satellite constellation market booms thanks to growing demand for global coverage. Available at: https://www.thalesgroup.com/en/worldwide-space/telecommunications/magazine/satellite-constellation-market-booms-thanks-growing (Accessed: 18 December 2019).

The Royal Society (2007) Detecting nuclear and radiological materials - RS Policy Document 07/08. Available at: https://royalsociety.org/~/media/royal_society_content/policy/publications/2008/7957.pdf (Accessed: 11 December 2019).

Trigo, I. F. *et al.* (2008) 'Thermal land surface emissivity retrieved from SEVIRI/Meteosat. In: IEEE Transactions on geoscience and remote sensing, pp. 307–315. https://doi.org/10.1109/TGRS.2007.905197.

Trigo IF et al (2011) The satellite application facility for land surface analysis. Int J Remote Sens 32(10):2725–2744. https://doi.org/10.1080/01431161003743199

UK Government (2016) MOD buys third record-breaking UAV-GOV.UK. Available at: https://www.gov.uk/government/news/mod-buys-third-record-breaking-uav (Accessed: 4 March 2020).

UK Government (2017) Technology that's out of this world - Cleaning up our nuclear past: faster, safer and sooner, gov.uk. Available at: https://nda.blog.gov.uk/2017/12/07/technology-thats-out-of-this-world/ (Accessed: 11 December 2019).

University of Hamburg (2019) MODIS Land Surface Albedo. Available at: https://icdc.cen.uni-hamburg.de/1/daten/land/modis-landalbedo.html (Accessed: 28 January 2020).

Virgili-Llop, J. *et al.* (2014) Very Low Earth Orbit mission concepts for Earth Observation. Benefits and challenges. Available at: https://www.researchgate.net/publication/271499606_Very_Low_Earth_Orbit_mission_concepts_for_Earth_Observation_Benefits_and_challenges (Accessed: 18 December 2019).

Walsh, J. A. and Berthoud, L. (2016) Is it possible to integrate electric propulsion thrusters on very-low earth orbit microsatellites? Available at: http://www.bristol.ac.uk/pure/user-guides/explore-bristol-research/ebr-terms/ (Accessed: 19 November 2020).

Walsh, J. A. and Berthoud, L. (2017) Reducing spacecraft drag in Very Low Earth Orbit through shape optimisation. https://doi.org/10.13009/EUCASS2017-449.

Wojtas, W. and European Commission DG Home Affairs (2018) Preparedness against CBRN threats-EU Action Plan Athens, Greece BEST PRACTICES IN IMPLEMENTING INTERNATIONAL HEALTH REGULATIONS (IHR) Wiktor WOJTAS Commission DG Home Affairs. Available at: https://eody.gov.gr/wp-content/uploads/2019/01/Wiktor_Wojtas_DG_HOME.pdf (Accessed: 13 November 2019).

World Meteorological Organisation (2020) WMO OSCAR. Available at: https://www.wmo-sat.info/oscar/ (Accessed: 3 November 2020).

World Nuclear Association (2020) Fukushima Daiichi Accident. Available at: https://www.world-nuclear.org/information-library/safety-and-security/safety-of-plants/fukushima-accident.aspx (Accessed: 6 December 2019).

Yelamanchili, A. *et al.* (2019) Mission analysis for EMIT using automated coverage scheduling CLASP for automated coverage scheduling: observation design and coverage strategy. Available at: www.nasa.gov (Accessed: 28 February 2020).